# Magnetic field evolution and reconnection in low resistivity plasmas

Allen H Boozer
*Columbia University, New York, NY 10027*
*ahb17@columbia.edu*
(Dated: February 3, 2023)

The recognized challenges of a driven evolution of a magnetic field are addressed in its three aspects: field line topology, magnetic energy, and magnetic helicity. Magnetic field lines can go from a simple smooth form to having large and broadly-spread changes in their connections on a timescale that is approximately a factor of ten longer than the ideal evolution time when and only when the magnetic field lines become chaotic. Footpoint motions transfer magnetic energy to coronal loops, which can only be balanced by highly localized current densities $j \approx vB/\eta$, where $v$ is the footpoint velocity and $\eta$ is the plasma resistivity. These current densities are consistent with those required to produce the solar corona with the observed height of the transition region through the Dreicer electron runaway effect. A small resistivity cannot balance the magnetic helicity input by footpoint motion and leads to the eruption of coronal loops.

## I. INTRODUCTION

According to Wikipedia: *Magnetic reconnection is a physical process occurring in highly conducting plasmas in which the magnetic topology is rearranged and magnetic energy is converted to kinetic energy, thermal energy, and particle acceleration.*

By definition, a highly conducting plasma plasma has a magnetic Reynolds number,

$$R_m \equiv \frac{\mu_0 v a}{\eta}, \tag{1}$$

that is far larger than unity; $v$ is a typical plasma flow speed, $a$ a typical spatial scale across the magnetic field, and $\eta/\mu_0$ is the resistive diffusion coefficient. In problems of interest $R_m$ can be between $10^4$ and $10^{14}$.

Magnetic topology rearrangement and magnetic energy conversion are distinct physical concepts, but each concept has been used to define magnetic reconnection. The classical definition was in a 1956 paper of Parker and Krook [1]: *severing and reconnection of lines of force*. In the space sciences, the emphasis has focused on energy conversion. In 2020, Hesse and Cassak stated [2]: *Magnetic reconnection converts, often explosively, stored magnetic energy to particle energy in space and in the laboratory.*

A practical understanding of magnetic field evolution when the magnetic Reynolds number, $R_m$, is large requires understanding the evolution of three distinct concepts: (i) magnetic topology, (ii) magnetic energy, and (iii) magnetic helicity. The nature of the evolution of these three concepts is frequently discussed in terms of two physical mechanisms: (1) the plasma flow velocity $\vec{v}$ and (2) the resistive diffusion of the magnetic field lines. Their relative magnitude is measured by the magnetic Reynolds number. Although many other mechanisms can affect the evolution, an understanding of reconnection using $\vec{v}(\vec{x},t)$ and $\eta/\mu_0$ is extremely informative.

There are two basic paradigms for magnetic reconnection. The classic paradigm is that of narrow sheets of intense current. Schindler, Hesse, and Birn [3] noted that

$$\frac{\partial \vec{B}}{\partial t} = \vec{\nabla} \times \left( \vec{v} \times \vec{B} - \eta \vec{j} \right) \tag{2}$$

implies that resistive breaking of the magnetic field lines directly competes with an evolution velocity $\vec{v}$ when the current density reaches an amplitude

$$j_{shb} \equiv \frac{vB}{\eta}. \tag{3}$$

This current density is $R_m$ times larger than the characteristic current density $B/\mu_0 a$, which implies the current must flow in a narrow sheet of cross-sectional area $a^2/R_m$. The length of the sheet is of order $a$ and the width is of order $a/R_m$. The classic reconnection paradigm of Schindler et al was developed for reconnection in which the magnetic field has a non-trivial dependence on only two spatial coordinates. The three dimensional case is the one of practical interest, but most of the literature is focused on two dimensions.

Magnetic field lines are chaotic when infinitesimally separated lines increase their separation exponentially with distance along the lines while remaining in a bounded region perpendicular to the magnetic field. Chaos, which is sometimes called magnetic stochasticity, is only possible when the magnetic field depends non-trivially on all three spatial coordinates.

A judgment of the importance of current sheets and chaos in understanding reconnection and magnetic evolution requires a list questions that need to be addressed. Such a list was provided in 2020

by one hundred eight members of the world reconnection community [4], who enumerated nine major challenges to understanding magnetic reconnection. Their list is copied into Appendix A and numbered by C1 to C9. Magnetic reconnection was defined as *the topological rearrangement of magnetic fields*. *Energy conversion* was a challenge, C3.

Here we explicitly show how chaos and other physics concepts developed in this and earlier papers address these challenges. The nine challenges can be studied analytically or through simulations. Unfortunately, numerical resolution becomes challenging when $R_m \gtrsim 10^4$, which is far smaller than Reynolds numbers of practical interest. Analytic understanding tested by simulations is required.

The implications of a given simulation on the various challenges can be subtle. This is illustrated by a model of a coronal loop driven by footpoint motions, Figure 1.a from Boozer and Elder [5]. This model allows a rigorous monitoring of *the topological rearrangement of magnetic fields*, and gives an exact expression for the minimum exponentiation of infinitesimally separated field lines in going from one footpoint to the other.

The most complete numerical study of the importance of chaos and current sheets to reconnection was described in a *Featured article* in the Physics of Plasmas, the simulations of Huang and Bhattacharjee [6]. They used the model of Figure 1.a to study two challenges: C5, *Onset* and C3, *Energy conversion*. With $R_m = 10^4$, they found the breaking of field line connections had reached 30% of the size of the top surface when the exponentiation of field-line separation approached $10^5$. Following Boozer and Elder, Huang and Bhattacharjee simplified the interpretation of the simulations by chosing the footpoint velocity $\vec{v}_t$ so no helicity is injected and the ideal, $R_m = \infty$, evolution is stable to kinks.

The reason for large-scale connection breaking when the exponentiation is larger than $R_M$ is intuitively obvious. Figure 1.b shows the distortion of tubes of magnetic field lines that Huang and Bhattacharjee observed for an ideal evolution when he exponentiation was much smaller than $10^5$. As the distortion of the tubes becomes ever greater, an arbitrarily small resistive diffusivity, $\eta/\mu_0$, can intermix the magnetic fields from different tubes, which changes the field line connections.

As will be shown in Sections IV B and V A 3, once field-line breaking is large-scale in the model of Figure 1.a, the current density can quickly rise to a value comparable to $j_{shb}$ at which resistivity can balance the power input from the footpoint motion. The Huang-Bhattacharjee simulations also showed this. Nevertheless, they interpreted the current density required for power balance as defining the true

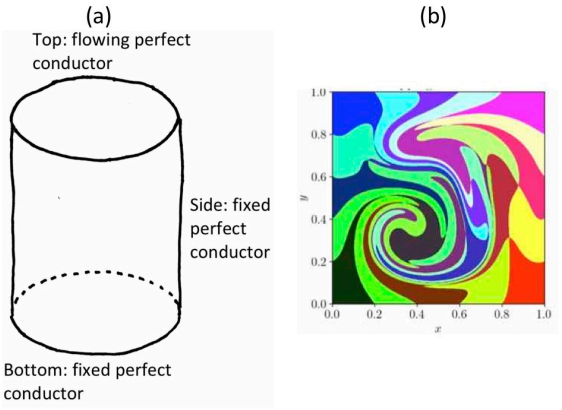


FIG. 1: (a) A perfectly conducting cylinder of height $L$ and radius $a$ encloses an ideal pressureless plasma. All of the sides of the cylinder are fixed except the top, which flows with a specified velocity $\vec{v}_t$. Initially, $\vec{B} = B_0\hat{z}$. Each point $\vec{x}_b$ on the bottom of the cylinder defines a line of $\vec{B}$ that in an ideal evolution intercepts a specific point on the top $\vec{x}_t$ with $\partial\vec{x}_t(\vec{x}_0,t)/\partial t = \vec{v}_t(\vec{x}_t,t)$ and $\vec{x}_0 \equiv \vec{x}_t$ at $t = 0$. The case of primary interest is when $\vec{v}_t$ is divergence free and chaotic. This means the $2\times 2$ Jacobian matrix $\partial\vec{x}_t/\partial\vec{x}_0$ has a large singular value that increases exponentially in time and a small singular value that is the inverse of the large singular value. This figure was originally published in Reference [5]. (b) Huang and Bhattacharjee [6] used an equivalent square-cylindrical model to project images on the top boundary of square tubes of magnetic field lines on the bottom boundary. As the distortions become ever larger, an arbitrarily small resistive diffusion $\eta/\mu_0$ can intermix field lines from different tubes and thereby change their connections. This figure is part of Figure 5 of their paper.

reconnection. The onset of large scale topological changes was interpreted as resistive diffusion—not reconnection.

Since the 1984 paper by Aref [7], it has been appreciated that the effect of stirring on mixing in fluids can only be understood by considering chaos—whether coffee and cream, a can of paint, a pot of soup, or temperature in a room. Both mixing in fluids and magnetic evolution are described by equations of the advection-diffusion type. Aref's analyzed the problem in Lagrangian coordinates, although the full equation was not written in Lagrangian coordinates until fifteen years later by Tang and Boozer [8]. The analysis applies to all equations of the advection diffusion type. Equation (2) for the magnetic evolution can be written in this form

$$\frac{\partial\vec{B}}{\partial t} - \vec{\nabla}\times(\vec{v}\times\vec{B}) = \frac{\eta}{\mu_0}\nabla^2\vec{B} \qquad (4)$$

by letting $\vec{j} = \vec{\nabla}\times\vec{B}/\mu_0$ and noting that $\vec{\nabla}\times(\vec{\nabla}\times\vec{B}) = -\nabla^2\vec{B}$. The left side of Equation (4) gives the

advection of $\vec{B}$ and the right side the diffusion. Note $\vec{\nabla} \times (\vec{v} \times \vec{B})$ equals $-\vec{v} \cdot \vec{\nabla} \vec{B}$ plus terms that ensure $\vec{\nabla} \cdot \vec{B}$ remains zero. The magnetic Reynolds number is called the Péclet number in scalar advection-diffusion problems, such as temperature relaxation $\partial T/\partial t + \vec{v} \cdot \nabla T = D_T \nabla^2 T$.

Trying to understand magnetic reconnection when the magnetic Reynolds number is large while ignoring chaos is in defiance of mathematics and intuition. It is as hopeless as ignoring chaos while trying to understand mixing in fluids at large Péclet numbers. Nevertheless, the effect chaos on magnetic evolution is subtle because chaos has a direct effect only on topological evolution and not on energy or on helicity dissipation.

The logarithm of the magnetic Reynolds number, $\ln R_m$, is of order of magnitude ten even when it is extremely large. This leads to a one-sentence statement of the importance of chaos to magnetic reconnection.

> **Magnetic field lines can go from a simple smooth form to having large and broadly-spread changes in their connections on a timescale that is approximately a factor of ten longer than the ideal evolution time when and only when the magnetic field lines become chaotic.**

This sentence about chaos could be shown to not be generally valid in two ways: (1) Find an evolving highly chaotic magnetic field that nonetheless preserves well-defined magnetic field line connections. (2) Find an evolving non-chaotic magnetic field that nonetheless goes from being simple and smooth to large scale connection breaking on a timescale only an order of magnitude longer than the ideal evolution time, even when $R_m$ is many orders of magnitude larger than unity.

This statement about the importance of chaos can never be proven to be correct. Karl Popper, one the twentieth century's most influential philosophers of science, famously stated [9] that no scientific statement can be proven to be correct but that it must in principle be testable. The most reliable scientific statements have been tested and never proven false.

The sentence about chaos has direct implications for five of the nine challenges in the list copied in Appendix A: C1, *The multiscale problem*; C2, *The 3D problem*; C5, *Onset*; C7, *Flow-driven*; and C9, *Related explosive phenomena*.

Section II, *History of chaos and reconnection* is a brief historical review of the realization of the importance of chaos to topological changes in magnetic field lines. The role of chaos in the evolution of magnetic fields is, however, subtle since its direct effect is limited to the breaking of field line connections.

Section III discusses two highly cited papers that should have fundamentally changed reconnection theory almost forty years ago. Nevertheless, they are rarely if ever referenced by the 108 authors [4] that listed the nine challenges: (1) A 1981 paper by Boozer [10] gave a general mathematical representation of the electric field, which separates connection-breaking from non-breaking terms. This paper is highly cited because it also demonstrated the existence of a coordinate system, now known as Boozer coordinates, which were the basis for solving what was thought to be a fatal flaw of stellarators, bad particle-trajectory confinement. (2) The 1984 paper by Aref that explained how stirring exponentially enhances mixing using to chaos, which applies to all evolution equations that are of the advection-diffusion form.

Section IV considers the evolution equations for magnetic topology, energy, and helicity. This section explains why chaos can exponentially shorten the time required for topological evolution but has no direct effect on energy or helicity evolution other than their spreading across a chaotic region. Sheets of concentrated current, which can rapidly dissipate the magnetic energy, are shown to be necessary to balance the energy input into coronal loops by footpoint motion, but have no effect on helicity evolution other than spreading. When footpoint motion inputs magnetic helicity, eruption of the loop is the only way it can be limited.

Section V is on the rate with which the current density can increase. In three dimensions, but not two, magnetic field lines can become chaotic without increasing the magnetic energy. The current density is increased by the exponential separation of the magnetic field lines, but need increase only algebraically, which means it is bounded by a constant times time $t$ to a power. The breaking of field line connection does not always release a large fraction of the stored magnetic energy into Alfvén waves. When it does, it is shown how the current density can rapidly rise in thin sheets to cause a rapid dissipation of the Alfvén wave energy.

Section VI discusses the formation of the solar corona by the Dreicer runaway mechanism due to the current density required for coronal power balance.

Section VII, Discussion, gives an overview of reconnection in toroidal and in space and astrophysical plasmas as well as the importance and difficulty of changing reconnection paradigms.

Appendix A gives the list of nine reconnection challenges written [4] by a hundred eight members of the word reconnection community.

Appendix B discusses the expression of Huang and Bhattacharjee [6] for the increase in the current density that is analogous to the expression given in Section V A.

## II. HISTORY OF CHAOS AND RECONNECTION

In three dimensions, the evolution of the velocity perpendicular to the magnetic field, the $\vec{v}_\perp$ part of $\vec{v}$ of Equation (2), typically causes the e-folding distance of magnetic field lines to become shorter as time increases. The natural scaling of the time required for large-scale breaking of field line connections to occur is then $(a/v_\perp)\ln(R_m)$ as $R_m \to \infty$. This phenomenon is discussed in a number of papers by Boozer, most recently [11–13], and by Boozer and Elder [5].

Many other authors have also recognized the fundamental importance of chaos In 2005, Borgogno, Grasso, Porcelli, Califano, Pegoraro, and Farina showed that the interaction of tearing modes with different helicities in toroidal plasmas creates magnetic field chaos and fundamentally changes the definition of magnetic reconnection from the case in which the magnetic field depends on only two spatial coordinates [14]. In 1999, Lazarian and Vishniac [15] and in 2011, Eynick, Lazarian, and Vishniac [16] disussed the role of chaos the theory of turbulent magnetic reconnection. This topic was reviewed by Lazarian, Eyink, Jafari, Kowal, Li, Xu, and Vishniac [17] in 2020. Turbulent systems are always chaotic, but chaotic systems need not be turbulent. As explained in the Introduction to [11], turbulence slows the effects of chaos as compared to smooth flows with the same speed. Eric Priest is associated with a large body of work on three-dimensional structures that tend to concentrate currents and thereby lead to enhanced reconnection [18]. In particular, he is known for his work on quasi-separatrix layers, which are essentially regions of field line chaos. Reid, Parnell, Hood, and Browning [19], have simulated a case in which the footpoint motions of magnetic field lines do not directly make the lines chaotic but drive large-scale instabilities that do. Huang and Bhattacharjee [6] recognize that magnetic fields that depend on all three spatial coordinates are generically chaotic and that the chaos makes the maintenance of field line connections fragile.

Evolving boundary conditions, such as footpoint motion of coronal magnetic field lines, can inject energy into the magnetic field. The breaking of field lines connections can release this energy from the large scale magnetic field but does not dissipate it. The obvious repository is Alfvén waves, which as will be shown can increase the maximum current density to the approximate value of Schindler et al, $j_{shb}$ required for resistive dissipation. A far smaller value of the current density is associated with large scale breaking of magnetic field-line connections, a density that depends logarithmically, not linearly, on $R_m$.

The motions of the footpoints can also inject magnetic helicity. As discussed in Boozer and Elder [5], the injected helicity dissipation is neither enhanced by chaos nor by intense currents flowing in thin sheets. When $R_m \to \infty$, the only way the injected helicity can be removed is by the ejection of coronal loops.

In toroidal plasmas, perturbations can distort the magnetic surfaces and cause rapid large-scale reconnections called disruptions. But, these perturbations neither inject magnetic helicity nor significant energy. As discussed by Boozer in 2022, the magnetic surfaces can become so contorted [20] that the separation between neighboring magnetic surfaces can vary by an exponentially large amount and cause the breaking of surfaces even as $R_m \to \infty$. This paper motivated a 2022 simulation by Jardin et al [21] that showed the limitation on the electron temperature in a spherical tokamak could be explained by ideal MHD instabilities sufficiently contorting magnetic surfaces to cause breaking despite the smallness of the resistivity. These results address challenge C4, Boundary conditions, in the list copied in Appendix A.

## III. IMPORTANT BUT OLD PAPERS

Two papers published approximately forty years ago should have fundamentally changed the theory of reconnection: (1) A general representation of $\vec{E}$ given by Boozer [10] in 1981, which implies Faraday's law for the evolution of the magnetic field lines is of the advection diffusion type. (2) Hassan Aref's paper [7] in 1984 that showed that equations of the advection-diffusion mathematical type generically have the diffusive effects exponentially enhanced by the chaotic properties of the advection, Section III B.

### A. General representation of $\vec{E}$

The theory of reconnection is greatly simplified when a distinction is made between the velocity $\vec{u}_\perp$ of the natural frame of reference of the magnetic field and the velocity $\vec{v}$ of the plasma. When the magnetic evolution is ideal, $\vec{u}_\perp$ is the velocity of the field lines, which cannot change their topology. The most profound implication of the introduction of the

velocity $\vec{u}_\perp$ is that Faraday's law is then shown to be of the advection-diffusion type for the evolution of the magnetic field lines, Equation (7). In the Introduction, Equation (2) was shown to be of the advection-diffusion type, Equation (4), but that was for the fluid velocity $\vec{v}$ while Equation (7) is for the velocity $\vec{u}_\perp$ of the magnetic frame of reference.

The velocity $\vec{u}_\perp$ of the natural frame of reference of the magnetic field is defined by a general representation of the three vector components of the electric field $\vec{E}$. The components can be represented in terms of a velocity $\vec{u}_\perp$ perpendicular to the field, a single-valued scalar potential $\Phi$, and $\mathcal{E}$, which is constant along a field line [10, 20],

$$\vec{E} + \vec{u}_\perp \times \vec{B} = -\vec{\nabla}\Phi + \mathcal{E}\vec{\nabla}\ell. \tag{5}$$

$\mathcal{E}\vec{\nabla}\ell$, where $\ell$ is the distance along a field line, is replaced in a torus by $(V_\ell/2\pi)\vec{\nabla}\varphi$. The field-line constant $V_\ell$ is the loop voltage and $\varphi$ is the toroidal angle.

Equation (5) is mathematical statement. Its validity requires only that the three components of $\vec{E}$ can be represented by $\Phi$, $\mathcal{E}$, and $\vec{u}_\perp$. Where $\vec{B}$ is non-zero, this can be simply demonstrated. The $\vec{B}\cdot\vec{E}$ component gives an equation for $\vec{B}\cdot\vec{\nabla}\Phi = B\partial\Phi/\partial\ell$, which can always be solved locally for $\Phi$. This solution may not be globally valid for a single-valued $\Phi$ in a torus or due to boundary conditions at the two ends of a field line. The field line constant $\mathcal{E}$ or $V_\ell$ resolves this issue.

The demonstration of the validity of Equation (5) is more subtle at places where $\vec{B} = 0$. An analytic function $\vec{B}(\vec{x})$ cannot be zero throughout a non-vanishing volume and not be zero everywhere—a Taylor series calculated in the non-vanishing volume is zero. $\vec{B}(\vec{x})$ can be zero along a line, but an arbitrarily small perturbation can change a line null into well-separated point nulls—only point nulls are generic. An infinitesimal sphere can be placed around each point null, then $\vec{B}(\vec{x}) \neq 0$ in the volume outside these spheres, which allows Equation (5) to be derived within that volume. Each infinitesimal sphere provides a boundary condition $\oint \vec{j}\cdot d\vec{a}$ to ensure charge does not accumulate at the null. This boundary condition determines $\Phi$ at the location of the null [22]. The important problem of magnetic reconnection in fields with point nulls produced by compact sources of magnetic fields was treated in 2019 by Elder and Boozer [23]. The issue of magnetic nulls and reconnection is not explicitly listed as a challenge in Appendix A, but C9, *The 3D problem*, mentioned interacting *flux ropes,* which are sometimes thought to be tubes with a strong magnetic field inside and essentially none outside. This is a difficult state to realize when the inner/outer field ratio is large and force balance is taken into account.

In 1958, Newcomb proved [24] that when $\mathcal{E} = 0$ the magnetic field lines move with the velocity $\vec{u}_\perp$ and their topology is conserved. When $\mathcal{E} \neq 0$, the magnetic field lines change topology by interchanging identities, so a field-line velocity cannot be defined. Nonetheless, $\vec{u}_\perp(\vec{x},t)$ defines a useful magnetic frame of reference.

Equation (5) is fundamentally different from an Ohm's law such as

$$\vec{E} + \vec{v}\times\vec{B} = \eta\vec{j} - \frac{\vec{\nabla}p_e}{en}; \tag{6}$$

the term $\vec{\nabla}p_e/en$ is called the Hall term. Ohm's law is a statement of physics, a constitutive relation, that gives one physical quantity, $\vec{E}(\vec{x},t)$ in terms of others, such as the mass flow velocity $\vec{v}(\vec{x},t)$, and the current density $\vec{j}(\vec{x},t)$ of a plasma. Terms in Ohm's law, such as $\eta\vec{j}_\perp$, the Hall term, and the friction from neutrals, cause the plasma velocity $\vec{v}$ to differ from $\vec{u}_\perp$ but clearly have no direct effect on changes in the topology of the magnetic field lines—only effects that produce a non-zero $\mathcal{E}$ can.

A number of the challenges enumerated in Appendix A are addressed or their interpretation changed by Equation (5): C4, *Boundary conditions*, C6, *Partial ionization*, and C9, *Related explosive phenomena*. C1, *The multiple scale problem*, has different interpretations when the magnetic velocity $\vec{u}_\perp$ is distinguished from the plasma velocity $\vec{v}$.

The most profound implication of Equation (5) is that when it is inserted into Faraday's Law the equation for the evolution of magnetic field lines

$$\frac{\partial\vec{B}}{\partial t} = \vec{\nabla}\times\left(\vec{u}_\perp\times\vec{B} - \mathcal{E}\vec{\nabla}\ell\right) \tag{7}$$

is of the advection-diffusion type. $\mathcal{E}$ is a field line average of $\eta\vec{j} = (\eta/\mu_0)\vec{\nabla}\times\vec{B}$; just as in Equation (4) this leads to a diffusive term $(\eta/\mu_0)\nabla^2\vec{B}$, which intermixes magnetic field lines interchanging their connections.

### B. Chaos and mixing

The chaos in flows has underlain the theory of fluid mixing since the famous 1984 paper of Hassan Aref [7]. The ubiquity of chaos is tested whenever one stirs coffee and cream, a can of paint, or a pot of soup. Chaos shorten the time for a radiator to heat a room from weeks to tens of minutes. For these examples, it is critical that the flow be driven throughout the region to be mixed. Otherwise, chaos is so ubiquitous that no special training

in the use of a stirrer is required—even slow stirring works as long as a flow is produced throughout the region to be mixed. Aref's paper on chaos and mixing is important whenever the underlying mathematical equation is of the advection-diffusion type and the diffusive term is small compared to the advective. Faraday's law is of this type.

### 1. *The ubiquity of chaotic flows*

The streamlines of a flow, $\vec{x}(\vec{x}_0, t)$, are defined by $d\vec{x}/dt = \vec{v}(\vec{x}, t)$ with $\vec{x}_0 \equiv \vec{x}(\vec{x}_0, 0)$. A plasma flow is chaotic when neighboring streamlines separate exponentially in time even while remaining in a bounded region of space.

A remarkable, but fundamentally a mathematical, statement is that essentially all non-trivial flows $\vec{v}(\vec{x}, t)$ that depend on at least two spatial coordinates and time are chaotic. This is most easily seen for divergence-free flows in two dimensions. For such flows $\vec{v} = \hat{z} \times \vec{\nabla} h(x, y, t)$ and the streamlines are given by Hamilton's equations, $dx/dt = -\partial h/\partial y$ and $dy/dt = \partial h/\partial x$. When $\partial h/\partial t = 0$, $h(x, y)$ must be constant along trajectories, and a trajectory followed in time cannot come arbitrarily close to every $(x, y)$ point in a bounded region of space. When $\partial h/\partial t \neq 0$, the Hamiltonian $h(x, y, t)$ changes along trajectories, which allows particle to come arbitrarily close. This is a signature of chaos.

A general theorem is that $h(x, y, t)$ is not chaotic when it is independent of any of the three variables $(x, y, t)$. Although there are no useful theorems about when the trajectories are chaotic, it is difficult to find non-trivial examples of $h(x, y, t)$ that are not—even when the dependence on the variables is smooth and on the spatial scale of the $x-y$ region in which the trajectories are bounded. Examples of simple, smooth, but chaotic flows are given in [5, 6] and in many other references. Although turbulent flows are chaotic, chaotic flows certainly need not be chaotic.

The standard example of a non-trivial $h(x, y, t)$ that is not chaotic is a twisting motion, but this tends to cause ideal kinking in plasmas, which leads to chaotic magnetic fields [5, 19].

### 2. *Chaos in $\vec{u}_\perp$ and $\vec{B}$ when $\mathcal{E} = 0$*

Even when $\mathcal{E} = 0$, a field-line flow $\vec{u}_\perp$ can take a magnetic field $\vec{B}$ with simple field line trajectories into one with chaotic field lines on the time scale of the flow.

Magnetic field lines are chaotic when neighboring pairs of lines separate exponentially when followed in distance along the lines. Flows are chaotic, when neighboring pairs of streamlines separate exponentially when followed in time.

The relationship between chaos in streamlines of $\vec{u}_\perp$ in time, and chaos in the lines of $\vec{B}$ in space, is clarified by the example given in Figure 1.a. The flow of the perfectly conducting top surface of the cylinder $\vec{v}_t$ is chaotic, but the perfectly conducting bottom surface is stationary. When a perfectly conducting plasma is enclosed by the perfectly conducting cylinder, tubes defined by magnetic field lines that enter the plasma at the bottom become increasingly distorted at the top as time advances, Figure 1.b. Neighboring magnetic field lines at the bottom have a separation at the top, which exponentially increases in time.

When boundary conditions on the magnetic field lines are given at the top and the bottom of the cylinder and $\mathcal{E} = 0$, a minimum level of exponentiation in separation is defined independent of the relationship between the plasma velocity $\vec{v}$ and the field line velocity $\vec{u}_\perp$. This has important implications for challenges C1, *The multiple scale problem*, C2, *The 3D problem*, C4, *Boundary conditions*, and C5, *Onset*, of Appendix A.

Three important points:

1. A magnetic field must develop a dependence on all three spatial coordinates for a field line flow $\vec{u}_\perp$ to cause the field lines to come arbitrary close to every point in a bounded region of space and be chaotic.

   The field line flow $\vec{u}_\perp$ must be two dimensional and time dependent to be chaotic. For the flow to make the field lines chaotic requires $\vec{B}$ lie in the direction of a third coordinate.

   This addresses challenge C2, *The 3D problem* in Appendix A.

2. An ideal evolution can cause perfect magnetic surfaces to become so contorted that a surface approaches arbitrarily closely every point in a non-zero volume of space [20].

   This addresses challenge C9, *Boundary conditions* in Appendix A and has important implications for ideal pressure-driven modes causing the breakup of magnetic surfaces in tokamaks [21] and other toroidal devices.

3. When $\ln R_m >> 1$, an important limitation [22] exists on the ratio of the length $L$ to width the width $a$ of coronal loops for the magnetic field lines to be sufficiently chaotic for the exponentiation to exceed the magnetic Reynolds number:

$$\frac{L}{a} \gtrsim \ln R_m. \tag{8}$$

Geometric constraints on rapidly reconnection regions are clearly of importance even though they are not mentioned in the nine fusion challenges. Simulations could study the way the constraint of Equation (8) manifests itself in the model of Figure 1.a when the height $L$ to radius $a$ ratio of the cylinder is small compared to $\ln R_m$. Do different chaotic regions define separate tubes that undergo reconnection of different time scales? Boozer and Elder [5] found the probability distributions for different levels of exponentiation, which means the fraction of the area of the top in which different levels of exponentiation arose; the median exponentiation is given by the square root of the maximum. It is not known whether this has a mathematical explanation.

The derivation of Equation (8) starts with the equation for the separation $\vec{\delta}$ between infinitesimally separated magnetic field lines $B\partial\vec{\delta}/\partial\ell = (\vec{\delta}\cdot\vec{\nabla})\vec{B}$. When the tensor $(\vec{\nabla}\vec{B})/B$ is much larger than the scale $a$, then its magnitude is of order $K \equiv \mu_0 j_{||}/B$. Let $d\sigma/d\ell = |\partial\vec{\delta}/\partial\ell|/|\vec{\delta}|$, then the number of e-folds of separation from a given field line $\sigma \approx \int K d\ell \approx KL$. The change in the magnetic field by the parallel current must be less than the total field, which implies $K\delta_\perp < 1$, where $\delta_\perp$ is the width of the current channel. Consequently, the length of the lines must satisfy $L > \sigma\delta_\perp$. For chaos to cause a sufficiently rapid changes in field line connections to compete with the evolution, $\delta_\perp$ must be less than $ae^\sigma/R_m$. The current channel width, $\delta_\perp$, must be less that the cross-field scale $a$, which implies $\sigma > \ln R_m$. The inequality $L/a \gtrsim \ln R_m$ follows.

Plasma resistivity causes magnetic fields to diffuse in space with a diffusion coefficient $\eta/\mu_0$. The distinction between field lines in a distorted tube of Figure 1.b and those in surrounding tubes cannot be made when the magnetic field can diffuse a distance comparable to the shortest distance across the tube. It is intuitively obvious that the preservation of magnetic field line connections, which is required in an ideal evolution, is lost once $\eta/\mu_0$ diffusion becomes this strong. This is analogous to the exponential enhancement of the mixing of fluids in chaotic flows famously pointed out in 1984 by Aref [7]. The precise relationship between fluid mixing and the breaking of field-line connections can be derived analytically [11]. The implication for the preservation of magnetic field line connections can be summarized in the boldface single sentence on page 3.

## IV. EVOLUTION OF MAGNETIC TOPOLOGY, ENERGY, AND HELICITY

### A. Conservation of magnetic field line topology

Both the conservation and the evolution of magnetic topology is rigorously defined by the magnetic field line Hamiltonian and its canonical coordinates. Applying a method, which is well known in toroidal plasmas [25], to the model of Figure 1.a, the magnetic field is written using $(\psi,\theta,z)$ as coordinates, which map $\vec{x}(\psi,\theta,z,t)$ to ordinary Cartesian coordinates as

$$\vec{x} = x(\psi,\theta,z,t)\hat{x} + y(\psi,\theta,z,t)\hat{x} + z\hat{z}; \tag{9}$$

$$\vec{B} = \frac{\vec{\nabla}\psi\times\vec{\nabla}\theta}{2\pi} + \frac{\hat{z}\times\vec{\nabla}\psi_p}{L}. \tag{10}$$

where $\psi$ is the longitudinal magnetic flux and $\psi_p((\psi,\theta,z,t)$ is the poloidal flux and the field line Hamiltonian,

$$\frac{d\psi}{\partial z} = -\frac{1}{L}\frac{\partial\psi_p}{\partial\theta} \quad \text{and} \quad \frac{d\theta}{\partial z} = \frac{1}{L}\frac{\partial\psi_p}{\partial\psi}. \tag{11}$$

The poloidal flux can be assumed to initially be zero, but it evolves according to the equation, appendix to [25],

$$\vec{E} + \vec{u}\times\vec{B} = \frac{\partial\psi_p(\psi,\theta,z,t)}{\partial t}\frac{\hat{z}}{L} - \vec{\nabla}\Phi, \quad \text{where} \tag{12}$$

$$\vec{u} = \frac{\partial\vec{x}(\psi,\theta,z,t)}{\partial t} \quad \text{with} \tag{13}$$

$$\vec{E} + \vec{u}\times\vec{B} = -\vec{\nabla}\Phi + \mathcal{E}(\psi,\theta,t)\hat{z}, \quad \text{so} \tag{14}$$

$$\frac{\partial\psi_p}{\partial t} = L\mathcal{E}. \tag{15}$$

Hamilton's equations for the magnetic field lines, Equation (11), change when and only when $\psi_p(\psi,\theta,z,t)$ changes. Consequently, the evolution of $\psi_p$ gives the topological evolution.

The equation $\vec{x}(\psi,\theta,z,t)$ maps the canonical coordinates of the magnetic field line Hamiltonian into Cartesian coordinates. When $\partial\psi_p/\partial t = 0$, the velocity $\vec{u} \equiv \partial\vec{x}/\partial t$ gives the velocity of the magnetic field lines through space.

The conservation of magnetic field topology is directly connected to the list of challenges in Appendix A since reconnection is defined as *the topological rearrangement of magnetic fields.*

### B. Energy evolution

Energy evolution is essentially challenge C3, *Energy conversion* in Appendix A.

### 1. General equations for power

Power is removed from the magnetic field at the rate $\vec{j}\cdot\vec{E}$. When $\vec{E}$ is given by the Ohm's law of Equation (6), then ignoring the Hall term

$$\vec{j}\cdot\vec{E} = \vec{v}\cdot(\vec{j}\times\vec{B}) + \eta j^2. \tag{16}$$

The term $\vec{v}\cdot(\vec{j}\times\vec{B})$ gives the transfer of energy to plasma, which is not in itself dissipative but can be dissipated by viscosity, Equation (31). The term $\eta j^2$ is the direct Ohmic dissipation of the magnetic energy.

The breaking of magnetic field line connections removes a constraint on magnetic evolution, but its connection with the transfer of energy from the magnetic field to the plasma is complicated. When the magnetic field evolution is ideal, the power transfer to the plasma is $\int \vec{v}\cdot(\vec{j}\times\vec{B})d^3x$. The $\vec{j}\times\vec{B}$ Lorentz force integrated over a thin current layer need not be large. A delta-function current density is equivalent to a current potential $\kappa$, which produces only a finite force on the current carriers [26]. A large power transfer occurs only when the flow velocity $\vec{v}$ is also concentrated in the thin layer.

When power is continuously put into the plasma, there are two ways it can be dissipated: by resistively $\int \eta j^2 d^3x$ and by viscosity $\int \rho\nu(\vec{\nabla}\times\vec{v})^2 d^3x$. An important but unsettled question is what fraction of the power is dissipated by viscosity versus resistivity in the limit as the magnetic Reynolds number $R_m \to \infty$. When the viscosity is extremely large, it would appear difficult to for the flow velocity to lie in thin layers, which seems necessary to form the thin layers of intense $j$ that are necessary for a large resistive dissipation. Is this true only when the fluid Reynolds number $R_f = av/\nu$ is less than unity? Or, can it be true when the Prandtl number $P_r = R_m/R_f = \mu_0\nu/\eta$ becomes sufficiently large even with $R_f >> 1$? Practical simulations can certainly determine the nature of reconnection for $R_f$ arbitrarily small, but practical limitations on the highest $R_m$ that can be simulated may prevent studies of the case with a very large Prandtl number but with $R_f > 1$. The role of viscosity in turbulent reconnection is addressed analytically in Jafari et al [27]. Resolution issues also limit simulation tests of viscosity effects in turbulent reconnection..

### 2. Power and coronal loops

Using the model of Figure 1, the power input of the footpoint motion is the power required to maintain the divergence-free flow in the top surface

$$\vec{v}_t = \hat{z}\times\vec{\nabla}h. \tag{17}$$

That power is the integral over the volume of the top surface,

$$\begin{aligned}
\mathcal{P}_f &= -\int \vec{v}_t\cdot(\vec{j}\times\vec{B})d^3x && (18)\\
&= \int B_z\vec{j}\cdot\vec{\nabla}h d^3x = B_0\oint h\vec{j}\cdot d\vec{a} && (19)\\
&= -\frac{B_0}{\mu_0}\int h(\vec{\nabla}\times\vec{B})\cdot\hat{z}da_t\\
&= -\frac{B_0}{\mu_0}\int \vec{\nabla}\times(h\hat{z})\cdot\vec{B}da_t\\
&= \frac{B_0}{\mu_0}\int \vec{v}_t\cdot\vec{B}_t da_t, && (20)
\end{aligned}$$

since $\vec{v}_t\cdot\vec{B} = \vec{v}_t\cdot\vec{B}_t$ with $\vec{B}_t$ the tangental magnetic field to the top surface.

The important equations for the power input are Equation (19), which gives the power using the stream function $h$ and the plasma current intercepting the top surface in Figure 1, and Equation (20), which gives the power using the velocity $\vec{v}_t$ of the top surface and the magnetic field tangent to that surface on the plasma side.

For resistive dissipation to balance the power input requires $\int \eta j_s^2 d^3x$ balance the power input $\mathcal{P}_f$ of Equation (19), where $j_s$ is the current density in a current sheet. Since $h \approx v_t a$,

$$\begin{aligned}
\mathcal{P}_f &\approx Bv_t a j_s A_s \approx \eta j_s^2 A_s L \ \text{ so} && (21)\\
j_s &\approx \frac{a}{L}\frac{Bv_t}{\eta} = \frac{a}{L}j_{shb} && (22)
\end{aligned}$$

where $A_s$ is the cross sectional area of the sheet current and $L$ is the height of the cylinder. The current $j_{shb}$ is defined in Equation (3). The factor $(a/L)B \approx \Delta B$ the change in the magnetic field required to track the moving interception point of a field line with the top surface when evolution is ideal, $\mathcal{E} = 0$. Although a current density as large as $j_{shb}$, which was defined by Schindler, Hesse, and Birn, is not required for chaos to allow large-scale reconnection, it is required for the resistive dissipation of the power input from footpoint motion.

## C. Helicity evolution

The robustness of magnetic helicity conservation has been known since the 1984 work of Berger [28]. The essential point is that the resistive change in the helicity is given by $\int \eta\vec{j}\cdot\vec{B}d^3x$, but resistive dissipation of energy is given by $\int \eta j^2 d^3x$. Concentrating the current in a thin channel enhances the energy dissipation but not the rate of helicity change. As discussed by Boozer and Elder when the timescale for helicity injection is shorter than the

resistive timescale defined by the spatially averaged parallel current, flux-tube eruption must eventually occur [5].

The role of helicity conservation in the space sciences is most prominent in the theory of dynamos, which is closely related to the theory of reconnection as noted in [4], Appendix A. The conservation properties of the helicity have been known since 1986 to invalidate the $\alpha$-effect dynamo [29]. A more detailed proof was given in 1995 by Bhattacharjee and Yuan [30]. Nevertheless, the $\alpha$-effect dynamo is commonly studied in dynamo simulations [31] by having a model that destroys helicity at small scales even though this is not energetically possible. A discussion of helicity conservation in dynamos in the presence of turbulence was given in 2011 by Vishniac and Cho [32].

The equation for magnetic helicity evolution was derived in Section VI of Reference [5] and is only summarized here. Letting $g(\vec{x},t)$ be the gauge of the vector potential,

$$\mathcal{K} \equiv \int \vec{A}\cdot\vec{B}d^3x \tag{23}$$

$$= \oint g\vec{B}\cdot d\vec{a} - \frac{2\int \psi_p d\psi d\theta dz}{2\pi L} \tag{24}$$

$$\frac{d\mathcal{K}}{dt} = \dot{K}_B - 2\int \mathcal{E}\frac{d\psi d\theta dz}{2\pi}, \quad \text{where} \tag{25}$$

$$\dot{K}_B = -2B_0^2\int h da_t \quad \text{so} \tag{26}$$

$$\frac{d\mathcal{K}}{dt} = -2B_0^2\int h da_t - 2\int \mathcal{E}\hat{z}\cdot\vec{B}d^3x \tag{27}$$

since the Jacobian of $(\psi,\theta,z)$ coordinates is $\mathcal{J} = 1/\hat{z}\cdot(\vec{\nabla}\psi\times\vec{\nabla}\theta) = 1/(2\pi\hat{z}\cdot\vec{B})$.

There are two important points. (1) Helicity is dissipated by the volume integral of $\mathcal{E}B_z$, so neither magnetic field line chaos nor the current density being concentrated into thin ribbons enhances its dissipation. (2) Helicity input occurs when $\int h da_t \neq 0$ in a single chaotic region. Using $(r_c,\theta_c,z)$ cylindrical coordinates, $\int h da_t = \int h r_c dr_c d\theta_c$. The implication is that only the $\theta_c$ average of the stream function $h$ contributes, which gives a purely circular flow pattern, $\bar{v}_{\theta_c}(r_c,t)\hat{\theta}_c$. A circular flow can drive ideal kink instabilities, Section IV of Reference [5], and cause the eruption of coronal loops. There is no alternative to an eruption when helicity is systematically accumulating in a loop.

Helicity evolution is central to the challenges C2, *The 3D problem*, and C9, *Related explosive phenomena* given in Appendix A.

## V. EVOLUTION OF THE CURRENT DENSITY

The increase in the current density along an arbitrarily chosen magnetic field line and the increase in the current density in a given flow are the two ways to estimate the rate the plasma current increases.

Surprisingly, the formation of current sheets and current densities comparable to $j_{shb}$ of Equation (3) is not mentioned in the list of challenges in Appendix A. Nevertheless, it enters many discussions about reconnection.

### A. Current density along an arbitrary line of $\vec{B}$

#### 1. *The near-line expansion*

A Taylor expansion near an arbitrarily chosen magnetic field line $\vec{x}_0(\ell,t)$, called the central line, gives the relation between the change in the twist of line with the distance along the line $\ell$ and the time derivative of the current density $j_{||}$ along the line [12].

The derivation uses the position vector $\vec{x}(\rho,\alpha,\ell) = \rho\cos\alpha\hat{\kappa}_0 + \rho\sin\alpha\hat{\tau}_0 + \vec{x}_0(\ell,t)$, where $\rho$ is the distance from the central line; $\hat{\kappa_0}$ and $\hat{\tau}_0$ are the curvature and torsion unit vectors of the cental line $\vec{x}_0(\ell,t)$. The trajectories of the adjacent lines are given by a $\tilde{H} = \tilde{\psi}h(\alpha,s)$, where $h = k_\omega(s,t) + k_q(s,t)\cos\left(2\alpha - \varphi_q(s,t)\right)$ with $k_\omega \equiv K_0/2 + \tau_0$. The magnitude of the quadrupole component of the magnetic field is given by $k_q\tilde{\psi}$, the only $\rho^2$ order Fourier component in the Hamiltonian. The magnetic flux is $\tilde{\psi} \equiv \pi B_0\rho^2$.

When the ideal evolution term, $\vec{v}\times\vec{B}$, is large compared to the resistive term, the evolution of the parallel current $j_{||}$ along an arbitrarily chosen magnetic field line $\vec{x}_0(\ell,t)$ is given by [12, 13]

$$\frac{\partial\Omega B_0}{\partial\ell} = \frac{\partial\left(K_0 + 2\tau_0 + \frac{4k_q^2}{\partial\varphi_q/\partial s}\right)B_0}{\partial t}. \tag{28}$$

$K_0(\ell,t) \equiv \mu_0 j_{||}/B_0$, $\Omega(\ell,t) = \hat{b}_0\cdot\vec{\nabla}\times\vec{v}$, and $\tau_0(\ell,t)$ is the torsion of the curve. The quantity $k_q^2/(\partial\varphi_q/\partial\ell)$ is defined by the quadrupole contribution to the Hamiltonian for the adjacent magnetic field lines and should only be retained when the adjacent field lines are not chaotic.

A more intuitive and more easily interpreted form of Equation (28) is

$$\frac{\partial\Omega B_0}{\partial\ell} = \frac{\partial\left(K_0 + 2\nu\right)B_0}{\partial t}, \tag{29}$$

where $\nu(\ell,t)$ is the stellarator-like rotational transform per unit length of field lines produced by currents at a distance from the chosen line. The term on the right-hand side of Equation (29) comes from the fact that when the externally-produced rotational transform $\nu$ per unit length has a positive time derivative, then $K_0$ must decrease to keep the total transform per unit length fixed. The factor of two comes from dependence of the current-produced transform at a radius $\rho_0$ being proportional to $(\int K\rho d\rho)/\rho_0^2 = K_0/2$ as $\rho_0 \to 0$. The left-hand side comes from the fact that when the field lines are undergoing a twist per unit time, which is what $\Omega$ is, then a current must increase to produce a total rotational transform per unit length that gives $\partial\Omega/\partial\ell$.

The term $\nu$ in Equation (29) represents the effects of distant currents. In principle, distant currents can produce chaos in a bounded region by themselves. For example, the magnetic surfaces in a curl-free stellarator can be perturbed to produce chaotic regions using additional curl-free fields that resonate with the rational surfaces. But, the term $\nu$ also represents the natural response of a perfectly conducting medium to a changing current. By Le Chatelier's principle that nature tends to resist change, one would expect a larger $K_0$ would be required to produce a given field line twist due to the presence of distant currents. Indeed, this is what was seen in the simulations of Huang and Bhattacharjee [6].

### 2. *Force-balance and plasma flow*

Once magnetic field lines have become chaotic, so connections are easily broken, the power input goes into plasma motion until it can be dissipated by resistivity or viscosity.

The divergence-free nature of the current $\vec{j}$ implies $K$ and the Lorentz force $\vec{f}_L \equiv \vec{j}\times\vec{B}$ are related by

$$\frac{\partial K}{\partial \ell} = \hat{b}\cdot\vec{\nabla}\times\frac{\mu_0\vec{f}_L}{B^2}, \text{ where} \quad (30)$$

$$\vec{f}_L = \rho\left(\frac{\partial\vec{v}}{\partial t}+\vec{v}\cdot\vec{\nabla}\vec{v}-\nu\vec{\nabla}\times\vec{\Omega}\right). \quad (31)$$

When the linear inertial term dominates $V_A^2\partial K/\partial\ell = \partial\Omega/\partial t$ and $K$ relaxes to being uniform along magnetic field lines at the Alfvén speed, $V_A$.

In principle, the distinction between the velocity of the plasma $\vec{v}$ and that associated with the magnetic field $\vec{u}$ could complicate the force-balance equation, but this distinction not generally not considered important in a near-ideal plasma.

### 3. *Increase in j due to Alfvén waves*

The current density required for breaking magnetic connections scales as $\ln R_m$ while the current density required to balance the power input into coronal loops by footpoint motion scales as $R_m$. The power released by the breaking of field line connections must initially go into Alfvén waves when $R_m$ is large and viscosity effects are small, as in the simulations of Huang and Bhattacharjee [6]. Consequently, the energy in Alvén waves increases until the current density reaches the value $j_s$, Equation (22), at which resistive dissipation can balance the power input $\mathcal{P}_f$ of the footpoint motion. Alfvén energy is evenly divided between magnetic and kinetic energy with the velocity and magnetic field fluctuations related by $\tilde{v}/V_A = \tilde{B}/B$ with $V_A$ the Alfvén speed.

The increase in the current density to the level the energy and Alfvén waves can be rapidly damped in essentially the topic of Alfvén wave damping in chaotic magnetic fields, which has been studied by several authors [33–35].

The field-line localized formula for the current density $\partial K/\partial t = \partial\Omega/\partial\ell$, where $K \equiv \mu_0 j/B_0$, predicts a rapid increase in the current density to the level $j_s$, or equivalently $K_s \equiv \mu_0 j_s/B_0 \approx R_m/L$, required to balance the input power due to the contribution of the Alfvén waves to the vorticity $\Omega$.

Once the velocity fluctuations $\vec{\tilde{v}}$ of the Alfvén waves are large, it is natural to expect $|\partial\vec{v}/\partial t| \approx |\vec{v}\cdot\vec{\nabla}\vec{v}| \approx \tilde{v}^2/\delta_{tan}$ where $\delta_{tan}$ is the scale of $\vec{\tilde{v}}$ variation along itself. This scale is much longer than the distance scale $\delta_\perp$ for $\vec{\tilde{v}}$ changes across the flow. This disparity in scales $\delta_{tan} >> \delta_\perp$ is related to the concentrated current lying in thin but broad ribbons along the magnetic field lines as seen by Boozer and Elder and predicted in [11] and illustrated in Figure 6 of Huang and Bhattacharjee's paper [6]. Since Alfvén waves propagate with the Alfvén speed, $|\partial\tilde{v}/\partial t| \approx (V_A/\delta_\ell)\tilde{v}$, with $\delta\ell$ the spatial scale parallel to B. Consequently, $\delta_\ell \approx (V_A/\tilde{v})\delta_{tan}$.

The contribution of Alfvén waves to the vorticity is $\Omega_A \approx \tilde{v}/\delta_\perp$, so $\partial\Omega_A/\partial\ell \approx \Omega_A/\delta_\ell$. The fraction of the cross sectional area occupied by the Alfvén waves and the sheets of intense current density is $f_A = \delta_\perp\delta_{tan}/a^2$, so

$$\frac{\partial\Omega_A}{\partial\ell} \approx \left(\frac{\tilde{v}}{V_A}\right)^2\frac{V_A}{f_A a^2} \quad (32)$$

$$\approx \left(\frac{\tilde{B}}{B}\right)^2\frac{V_A}{f_A a^2}. \quad (33)$$

The time required to set up the sheet current

$$K_s = \frac{\mu_0}{\eta}\frac{v_t a}{L} = \frac{R_m}{L} \text{ is} \quad (34)$$

$$\tau_s = \frac{K_s}{\partial\Omega_A/\partial\ell} \tag{35}$$

$$\approx \left(\frac{B}{\tilde{B}}\right)^2 \frac{f_A a^2}{V_A}\frac{R_m}{L} \tag{36}$$

$$\approx \left(\frac{aB}{L\tilde{B}}\right)^2 \frac{L}{V_A} \tag{37}$$

since $f_A R_m \approx 1$.

The Introduction to [22] explains why the magnetic perturbation perpendicular to the initial magnetic field reaches an amplitude $\Delta B \approx (a/L)\ln R_m$ when large scale reconnection commences. A large fraction of the associated magnetic energy goes into the Alfvén waves so time to build up the sheet current can be very short $\tau_s \approx (L/V_A)/(\ln R_m)^2$ compared to the time required to reach sufficient exponentiation $(a/v_t)\ln R_m$. The velocity of the footpoints $v_t$ is small compared to the Alfvén speed $V_A$ in problems of primary interest. Once large scale breaking of field line connections had occurred, the formation of sheet currents quickly followed in the simulations of Huang and Bhattacharjee citeHuang-Bhattacharjee.

### B. Current increase in a given flow

When the magnetic field lines have a known velocity, $\vec{u}_\perp(\vec{x},t)$, the Cauchy solution for the ideal evolution of the magnetic field is

$$\vec{B}\big(\vec{x}(\vec{x}_0,t)\big) = \frac{\overleftrightarrow{J}_L}{\mathcal{J}_L}\cdot\vec{B}(\vec{x}_0), \tag{38}$$

where $\overleftrightarrow{J}_L$ is the Jacobian matrix of the Lagrangian coordinates of $\vec{u}_\perp$ and $\mathcal{J}_L$ is the determinant of $\overleftrightarrow{J}_L$. The history of this solution was reviewed by Stern [36] in 1966.

Equation (38) has profound implications about the differences in between two and three dimensional evolution and the speed with which the current density can increase.

The Cauchy solution is a purely mathematical statement about Faraday's law, $\partial\vec{B}/\partial t = -\vec{\nabla}\times\vec{E}$, and the representation of the vector $\vec{E}$ in terms of $\vec{B}$ with $\mathcal{E}=0$. Widespread confusion exists within the reconnection community between this mathematical representation of $\vec{E}$ and Ohm's law, which is the constitutive expression for the electric field. This distinction is explained in Section III A.

Section V B 1 defines Lagrangian coordinates, $\vec{x}(\vec{x}_0,t)$, and explains the Singular Value Decomposition of the Jacobian matrix $\overleftrightarrow{J}_L \equiv \partial\vec{x}/\partial\vec{x}_0$. The implications of the Cauchy solution are discussed in Section V B 2.

#### 1. *Lagrangian coordinates*

Lagrangian coordinates $\vec{x}_0$ are defined so that the position vector in ordinary Cartesian coordinates is $\vec{x}(\vec{x}_0,t)$, where

$$\left(\frac{\partial\vec{x}}{\partial t}\right)_L \equiv \vec{u}_\perp(\vec{x},t) \text{ with } \vec{x}(\vec{x}_0,t=0)=\vec{x}_0. \tag{39}$$

The subscript "$L$" implies the Lagrangian coordinates $\vec{x}_0$ are held fixed.

The three-by-three Jacobian matrix of Lagrangian coordinates can be decomposed as

$$\frac{\partial\vec{x}}{\partial\vec{x}_0} \equiv \begin{pmatrix} \frac{\partial x}{\partial x_0} & \frac{\partial x}{\partial y_0} & \frac{\partial x}{\partial z_0} \\ \frac{\partial y}{\partial x_0} & \frac{\partial y}{\partial y_0} & \frac{\partial y}{\partial z_0} \\ \frac{\partial z}{\partial x_0} & \frac{\partial z}{\partial y_0} & \frac{\partial z}{\partial z_0} \end{pmatrix}$$
$$= \overleftrightarrow{U}\cdot\begin{pmatrix} \Lambda_u & 0 & 0 \\ 0 & \Lambda_m & 0 \\ 0 & 0 & \Lambda_s \end{pmatrix}\cdot\overleftrightarrow{V}^\dagger. \tag{40}$$

where $\overleftrightarrow{U}$ and $\overleftrightarrow{V}$ are unitary matrices, $\overleftrightarrow{U}\cdot\overleftrightarrow{U}^\dagger = \overleftrightarrow{1}$. The three real coefficients $\Lambda_u \geq \Lambda_m \geq \Lambda_s \geq 0$ are the singular values of the Singular Value Decomposition (SVD). The Jacobian matrix can also be written as

$$\frac{\partial\vec{x}}{\partial\vec{x}_0} = \hat{U}\Lambda_u\hat{u} + \hat{M}\Lambda_m\hat{m} + \hat{S}\Lambda_s\hat{s}, \tag{41}$$

where $\hat{U}$, $\hat{M}$, and $\hat{S}$ are orthogonal unit vectors, $\hat{U} = \hat{M}\times\hat{S}$, of the unitary matrix $\overleftrightarrow{U}$, which means they define directions in the ordinary space of Cartesian coordinates, $\vec{x}$. The unit vectors $\hat{u}$, $\hat{m}$, and $\hat{s}$ are determined by the unitary matrix $\overleftrightarrow{V}$, which means that they define directions in the space of Lagrangian coordinates, $\vec{x}_0$.

The Jacobian of Lagrangian coordinates, which is the determinant of the Jacobian matrix, is

$$\mathcal{J}_L = \Lambda_u\Lambda_m\Lambda_s. \tag{42}$$

The time derivative $\big(\partial\ln(J_L)/\partial t\big)_L = \vec{\nabla}\cdot\vec{u}_\perp$. For the model of Figure 1 a, the Jacobian changes little from unity.

The properties of evolving magnetic fields and currents using Lagrangian coordinates were discussed by Tang and Boozer [37] in 2000 and by Thiffeault and Boozer [38] in 2003.

#### 2. *Implications of the Cauchy $\vec{B}(\vec{x},t)$*

Using the Singular Value Decomposition of Lagrangian coordinates, Equation (38) for the Cauchy

solution implies [11]

$$B^2 = \left(\frac{\hat{u}^\dagger \cdot \vec{B}_0}{\Lambda_m \Lambda_s}\right)^2 + \left(\frac{\hat{m}^\dagger \cdot \vec{B}_0}{\Lambda_u \Lambda_s}\right)^2 + \left(\frac{\hat{s}^\dagger \cdot \vec{B}_0}{\Lambda_u \Lambda_m}\right)^2 . \quad (43)$$

The mathematical definition of a chaotic $\vec{u}_\perp$ is that the largest singular value $\Lambda_u > \exp(t/\tau_L)$ for some $\tau_L > 0$ for any time $t$ greater than a sufficiently large value. The smallest $\tau_L$ that satisfies this inequality gives the exponentiation timescale. The product of the three singular values $\Lambda_u \Lambda_m \Lambda_s \approx 1$. When $\Lambda_u$ increases exponentially, $\Lambda_s$ decreases exponentially, and $\Lambda_m$ has at most an algebraic dependence on time. The exponentiation time scale $\tau_L$ is usually comparable to the evolution time scale.

The term in $B^2$ proportional to $(\hat{u}^\dagger \cdot \vec{B}_0)^2$ goes to infinity exponentially in time. The term proportional to $(\hat{s}^\dagger \cdot \vec{B}_0)^2$ goes to zero exponentially. A bounded magnetic field strength is only possible for a time long compared to $\tau_L$ when the magnetic field points in the $\hat{M}$ direction,

$$\vec{B}(\vec{x}, t) \rightarrow \frac{\hat{m}^\dagger \cdot \vec{B}_0}{\Lambda_u \Lambda_s} \hat{M}. \quad (44)$$

The unit vector $\hat{M}$ is also the unit vector along the magnetic field $\hat{b}$. When the magnetic field is in the $\hat{M}$ direction the current density $\vec{j}$ lies in ribbons along the magnetic field lines which become exponentially wider and exponentially thinner in time with the magnitude of the current density increasing only algebraically [11]. The results of Boozer and Elder [5] in 2021 exhibit these properties as apparently does the ideal solution of Huang and Bhattacharjee [6].

Any smooth flow must naturally be consistent with the magnetic field lying in the $\hat{M}$ direction. Otherwise the magnetic field pressure $B^2/2\mu_0$ would increase exponentially in time.

The number of spatial dimensions is critical in reconnection theory because the number of singular values of Jacobian matrix equals the number of coordinates. In two dimensions, a chaotic $\vec{u}_\perp$ implies the magnetic field strength must increase exponentially in time, but not in three dimensions.

When $\vec{B}$ has a small component in the $\hat{U}$ direction, that component and the associated current density are amplified exponentially in time until that component becomes comparable to $\vec{B}$. The implication is that localized flows, which are seen in the Huang and Bhattacharjee simulations [6], can produce thin current sheets on a fast time scale as discussed in Section V A 3.

Although force-limits push $\vec{B}$ to be in the direction $\hat{M}$, which allows only an algebraic increase in current density with time, the small deviations in $\vec{B}$ that are associated with different current profiles can be in the exponentiating $\hat{U}$ direction, which has an exponentially increasing current density. This exponentiation can only hold while the current channel narrows while the spatially-averaged current density remains essentially constant.

## VI. RUNAWAY ELECTRONS AND THE CORONA

A large current density, of order $j_{shb}$, can be required to Ohmically dissipate the power input of the footpoint motion of coronal loops, Section IV B. This current density can exceed that required for electron runaway, the Dreicer current density $j_d$. When $j > j_d$, small-angle Coulomb collisions cannot maintain a near Maxwellian distribution, and electrons runaway to a high energy. The calculations of Kulsrud et al [39] imply the rate of electron runaway reaches a significant value at the current density $j_d = 2 \times 10^{-2} e n v_e$.

As pointed out by Boozer in [40] and discussed in [25, 41], when the Dreicer current is exceeded, electrons must runaway to whatever energy is required to carry the current. For the corona, this means to a sufficiently high energy that the electron density $n$ does not become too small due to the gravitational acceleration of the sun $g$. When the temperature $T$ is constant, $dn/dr = -n/h$, where the scale height $h \equiv T/Mg$. When the ionization is high, $M = m_i$, the proton mass, and $h \approx 350T$ km/eV. A coronal temperature of 100 eV is consistent with a scale height of 35,000 km.

Below the transition region to the corona, Song [42] found the electron temperature is almost constant, $\approx 0.5$ eV, which implies an electron thermal speed $v_e \approx 3 \times 10^5$ m/s and the Spitzer resistivity $\eta \approx 4 \times 10^{-3}$ Ohm-meter. The electron density drops rapidly with altitude above the photosphere and reaches $n \approx 3 \times 10^{16}/\mathrm{m}^3$, at the transition. The Dreicer current at the transition is then $j_d \approx 10^5$ A/m$^2$. The current density $j_{shb} \equiv vB/\eta \approx 250 vB$, which equals $j_d$ when $Bv \approx 400$ T·m/s. Song found the magnetic field is highly localized in flux tubes on the photosphere, but those tubes have large diameters at the transition region.

The magnetic field and velocity that should be used to estimate of $j_{shb}$ are uncertain. For coronal loops driven by sunspots, two papers are of particular importance. Okamoto and Sakurai [43] have observed fields above 0.6 T at sunspots, and Sobotka and Puschmann [44] have observed horizontal flows of 4 km/s. The product of these numbers gives $Bv = 2400$ T·m/s approximately six times higher than that required for $j_d = j_{shb}$ at the transition.

More typical velocities and fields could produce an exact balance.

As noted in [25], any star that has evolving magnetic field structures on the scale of tens of thousands of kilometers must have a corona, otherwise the induced currents would run out of current carriers, but whether this actually explains the solar corona requires careful study.

Although coronal heating is not directly mentioned among the challenges of Appendix A, it is connected with C3, *Energy conversion*, and C6, *Partial ionization*.

## VII. DISCUSSION

Coherent discussions of the challenges of magnetic reconnection require sensitivity to the definition of reconnection and the important questions. For that the ArXiv publication of 108 authors [4], which is quoted in Appendix A, is important. Nevertheless, different views about what are the important questions remain apparent between studies of toroidal magnetic-fusion plasmas and studies of space and astrophysical plasmas: (1) When the initial condition of an evolving magnetic field is smooth, is the time required for reconnection to occur on a timescale comparable to the timescale set by an evolution? This is a central issue in tokamak disruptions but the onset time for reconnection has not been a focus in space and astrophysical plasmas. (2) How should the speed of reconnection be defined? When rapid energy transfer from the magnetic field to the plasmas is the definition of reconnection then the rate of transfer provides a definition.

### A. Reconnection in toroidal plasmas

The periodicity of toroidal fusion plasmas gives a clear definition of the breaking of magnetic connections. Breaking connections means breaking magnetic surfaces, as in a tokamak disruption.

When a rapid breaking of the toroidal magnetic surfaces occurs in a tokamak, the definition of the speed of reconnection is subtle. Magnetic field lines are defined at points in time. When the last intact magnetic surface is broken, a magnetic field line at that instant changes from being bound by that surface to traversing the plasma and striking the chamber walls. The relevant speed is not defined by the instantaneous change in the trajectory of the field line but by the speed of physical effects that are produced by the topological change, the time it takes for particles or energy to be transported along magnetic field lines throughout a chaotic region. For $j_{||}/B$ flattening, the characteristic time is the time for shear Alfvén waves to cover the chaotic region by propagating along the magnetic field lines. The topological change can allow relativistic electrons trapped in the core of a tokamak to strike the surrounding walls by following magnetic field lines. The damage to the device is largely determined by how highly localized in space and time are the strikes of the relativistic electrons on the walls.

### B. Reconnection is space and astrophysical plasmas

In space plasmas the boundary conditions are often too indeterminate to rigorously define magnetic field line topology or what is meant by the breaking of field-line connections. Consequently, little study is done of the physical effects produced by the changes in field line connections. Yet, answers to physical questions within the region of interest may depend on what happens outside that region [47].

When topology and changes in field line connections are ill-defined, energy transfers between the field and the plasma seem most important, and it is natural to define magnetic reconnection by the energy transfer [2]. Energy transfer can be defined even in models in which changes in magnetic topology are not defined. Energy release from the magnetic field can occur even when $\eta = 0$; ideal magnetic kinks are a well known example. Nevertheless, the energy release from the magnetic field is generally greater when the field-line connections are freely broken. The direct energy release from the magnetic field is of little interest in the fast reconnections called tokamak disruptions for less than a part in a thousand of the energy is typically released [46].

Space and astrophysical studies are focused not only on the energy transfer from the fields to the plasma but also on acceleration of particles by the reconnection process. Although the acceleration of electrons to relativistic energies as a result of magnetic surface reconnection is a major issue in tokamaks, the acceleration is not a direct part of the reconnection process but rather a result of the plasma cooling increasing the resistivity to the point that $\eta\bar{j}$, with $\bar{j}$ a spatially-averaged current density, gives an electric field above that required for electron runaway. Electron runaway also offers a compelling explanation of the solar corona and serves as a check on the production of intense currents by even smooth, large-scale footpoint motion.

### C. Commonality of reconnection issues

The centrality of chaos to understanding changes in the topology of magnetic field lines seems clear when the evolution involves all three spatial coordinates. It is implied by a mathematical analysis of Faraday's law, by intuition based of pictures such as Figure 1 b, and by analogy to mixing in fluids.

By making the preservation of connections of magnetic field lines fragile, chaos can cause energy to be transferred from the large scale magnetic field to Alfvén waves. The damping of the Alfvén waves involves intense current sheets. The extent to which the fluid viscosity of the plasma can dissipate the energy released by the magnetic field requires more study. At a sufficiently large Prandtl number, $P_r \equiv \nu/(\eta/\mu_0)$, the ratio of viscosity to resistivity, the flows needed to produce the intense current sheets must be damped, but the level is presently unknown.

Neither magnetic field line chaos nor intense current sheets enhance the dissipation of magnetic helicity. Helicity input from footpoint boundary conditions cannot be dissipated in a low resistivity plasma, which makes helicity accumulation an obvious cause for eruption of coronal loops. Helicity conservation during the magnetic reconnection of tokamak disruptions, limits the release of energy from the magnetic field to extremely small values [46].

### D. Importance of chaos in reconnection literature

In 1962, Thomas Kuhn [48] in *one of the most influential works of history and philosophy written in the 20th century* [49], discussed how differences in the important questions and in the important features of a model arise whenever a new paradigm is introduced. He also pointed out how difficult it is for a scientific community to accept a change in paradigm.

Although the one sentence statement about chaos on page 3 should be tested, the fact that Faraday's law and the general expression for the electric field give an advection diffusion equation make failures unlikely in the extreme. Basing a reconnection theory on the failure of Maxwell's equations does not seem winning strategy. A change in the paradigm for rapid changes in magnetic topology is required from intense current sheets with $j \approx vB/\eta$ of the Schindler, Hesse, and Birn to the centrality of chaos.

Simulations of magnetic evolution with credible boundary conditions as the largest achievable magnetic Reynolds numbers are needed to guide the physics. Many issues could be better understood through practical simulations. A few of importance to solar physics are (1) the constraint $L/a \gtrsim \ln R_M$ on coronal loops, (2) the role of viscosity, (3) the extent to which Dreicer runaway explains the corona, (4) the constraints of solar footpoint flows that can be obtained from the behavior of coronal loops, (5) the effect of curvature on evolution of coronal loops.

Unfortunately, simulations do not have the numerical resolution to directly solve magnetic evolution problems with the largest magnetic Reynolds numbers of practical interest. These problems require an analytic understanding of evolution of the three physical concepts: magnetic topology, energy, and helicity.


### Acknowledgements

This work was supported by the U.S. Department of Energy, Office of Science, Office of Fusion Energy Sciences under Award Numbers DE-FG02-95ER54333, DE-FG02-03ER54696, DE-SC0018424, and DE-SC0019479.


### Data availability statement

Data sharing is not applicable to this article as no new data were created or analyzed in this study.

### Appendix A:

### Major Scientific Challenges and Opportunities in Understanding Magnetic Reconnection and Related Explosive Phenomena in Solar and Heliospheric Plasmas [4]

### I. Magnetic Reconnection: A Fundamental Process throughout the Universe and in the Lab

Magnetic reconnection—the topological rearrangement of magnetic fields—underlies many explosive phenomena across a wide range of natural and laboratory plasmas. It plays a pivotal role in electron and ion heating, particle acceleration to high energies, energy transport, and self-organization. Reconnection can have a complex relationship with turbulence at both large and small scales, leading to various effects which are only beginning to be understood. In heliophysics, magnetic reconnection plays a key role in solar flares, coronal mass ejections and heating, the interaction of the solar wind with planetary magnetospheres, associated dynamical phenomena such as magnetic substorms, and the behavior of the heliospheric

boundary with the interstellar medium. Magnetic reconnection is also integral to the solar and planetary dynamo processes. In short, magnetic reconnection plays a key role in many energetic phenomena throughout the Universe, including extreme space weather events that have significant societal impact and laboratory fusion plasmas intended to generate carbon-free energy.

## II. Major Scientific Challenges in Understanding Reconnection and Related Explosive Phenomena in Heliophysics

**C1. The multiple scale problem:** Reconnection involves the coupling between the fluid or MHD scale of the system and the kinetic ion and electron dissipation scales that are orders of magnitude smaller. This coupling is currently not well understood, and the lack of proper treatments in a self-consistent model is the core of the problem. Reconnection phase diagrams based on plasmoid dynamics clarify different possibilities for coupling mechanisms. Key questions include: how do plasmoid dynamics scale with key parameters, such as the Lundquist number and effective size; how is this scaling influenced by a guide field; do other coupling mechanisms exist; and how does reconnection respond to turbulence and associated dissipation on scales below or above the electron scales?

**C2. The 3D problem:** Numerous studies have focused on reconnection in 2D while natural plasmas are 3D. It is critical to understand which features of 2D systems carry over to 3D, and which are fundamentally altered. Effects that require topological analysis include instabilities due to variations in the third direction leading to complex interacting "flux ropes," potentially enhancing magnetic stochasticity, and field-line separation in 3D. How fast reconnection is rlated to self-organization phenomena such as Taylor relaxation, as well as the accumulation of magnetic helicity, remains a longstanding problem with important implications for, e.g., coronal heating and eruptions.

**C3. Energy conversion:** Reconnection is invoked to explain the observed conversion of magnetic energy to heat, flow, and to non-thermal particle energy. A major challenge in connecting theories and experiments to observations is the ability to quantify the detailed energy conversion and partitioning processes. Competing theories of particle acceleration based on 2D and 3D reconnection have been proposed, but as of yet there is no consensus on the origin of the observed power laws in particle energy distributions.

**C4. Boundary conditions:** It is unclear whether an understanding of reconnection physics in periodic systems can be directly applied to natural plasmas, which are non-periodic and often line-tied at their ends such as in solar flares. Whether line-tying and driving from the boundaries fundamentally alter reconnection physics has profound importance in connecting laboratory physics to heliophysics. It is also important to learn how reconnection works in naturally occurring settings that have background flows, out-of-plane magnetic fields, and asymmetries.

**C5. Onset:** Reconnection in heliophysical and laboratory plasmas often occurs impulsively, with slow energy build up followed by a rapid energy release. Is the onset a local, spontaneous (e.g., plasmoid instability) or a globally driven process (e.g., ideal MHD instabilities), and is the onset mechanism a 2D or 3D phenomenon? How do collisionality and global magnetic geometry affect the onset conditions? A related question is how magnetic energy is accumulated and stored prior to onset, e.g., in filament channels on the Sun and in the lobes of Earth's magnetotail.

**C6. Partial ionization:** Reconnection events often occur in weakly ionized plasmas, such as the solar chromosphere (whose heating requirements dwarf those of corona), introducing new physics from neutral particles. Questions include whether reconnection is slowed by increased friction or accelerated by enhanced two-fluid effects.

**C7. Flow-driven:** Magnetic fields are generated by dynamos in flow-driven systems such as stars and planets, and reconnection is an integral part of the dynamo process. Key questions include: under what conditions can reconnection occur in such systems; how fast does it proceed; how does reconnection affect the associated turbulence?

**C8. Turbulence, shocks, and reconnection:** Reconnection is closely interconnected to other fundamental plasma processes such as turbulence and shocks, which in turn produce heliophysical phenomena such as solar energetic particles. It is essential to understand the rates of topology change, energy release, and heating during reconnection, as they may be tied to the overall turbulence and shock dynamics.

**C9. Related explosive phenomena:** Global ideal MHD instabilities, both linear (kink, torus)

and nonlinear (ballooning), are closely related to reconnection either as a driver or a consequence (e.g., coronal mass ejections, magnetic storms/substorms, and dipolarization fronts in the magnetotail). Understanding how, and under what conditions, such explosive phenomena take place, as well as their impact, remain major scientific challenges. Physics insights from reconnection under extreme conditions in astrophysics should be beneficial as well.

### Appendix B: Current density increase of Huang and Bhattacharjee

Equation (15) of Huang and Bhattacharjee [6] appears to be analogous to Equation (29). Their analogue to $2\partial\nu(\ell,t)/\partial t$ is $\mathcal{T}$, where

$$\mathcal{T} \equiv \partial_x \vec{u}\cdot\partial_y \vec{B}_\perp - \partial_y \vec{u}\cdot\partial_x \vec{B}_\perp. \tag{B1}$$

Their paper emphasizes the importance of $\mathcal{T}$ to the differences between their results and those of Boozer and Elder [5].

Near a given line the divergence-free magnetic field line velocity and the ideal perturbation to the magnetic field $\delta\vec{B}$ can be written in terms of the field line displacement $\vec{\Delta}$ with $\vec{\nabla}\cdot\vec{\Delta}=0$;

$$\vec{u} = \frac{\partial\vec{\Delta}}{\partial t}; \tag{B2}$$

$$\delta\vec{B} = \vec{\nabla}\times(\vec{\Delta}\times B_0\hat{z}) \tag{B3}$$

$$= B_0\frac{\partial\vec{\Delta}}{\partial z}. \tag{B4}$$

The displacement is the sum of two parts: a part with a curl, $\vec{\Delta}_c$, and a quadrupole part, $\Delta_q$, that does not. Each has an associated velocity and perturbed magnetic field. The displacement $\Delta_c$ also has an associated vorticity $\Omega$ and a parallel current density, or $K$, but $\Delta_q$ does not.

$$\vec{\Delta}_c = \Delta_{c1}(z,t)x\hat{y} - \Delta_{c2}(z,t)y\hat{x}; \tag{B5}$$

$$\Omega \equiv \hat{z}\cdot\vec{\nabla}\times\vec{u}_c \tag{B6}$$

$$= \frac{\partial(\Delta_{c1}+\Delta_{c2})}{\partial t}; \tag{B7}$$

$$\frac{\delta\vec{B}_c}{B_0} = \frac{\partial\Delta_{c1}}{\partial z}x\hat{y} - \frac{\partial\Delta_{c2}}{\partial z}y\hat{x}; \tag{B8}$$

$$K \equiv \frac{\hat{z}\cdot\vec{\nabla}\times\delta\vec{B}_c}{B_0} \tag{B9}$$

$$= \frac{\partial(\Delta_{c1}+\Delta_{c2})}{\partial z}; \tag{B10}$$

$$\vec{\Delta}_q = \Delta_q(t)(x\hat{x}-y\hat{y})\cos(k_z z) + \Delta_q(t)(y\hat{x}+x\hat{y})\sin(k_z z); \tag{B11}$$

$$\delta\vec{B}_q = k_z B_0\Big\{(y\hat{x}+x\hat{y})\cos(k_z z) - (x\hat{x}-y\hat{y})\sin(k_z z)\Big\}. \tag{B12}$$

The magnetic scalar potential that gives the dipolar field is proportional to $\rho^2\cos(2\theta-k_z z)$, where $\rho$ is the distance from the line, and $\theta$ is the angle around the line. Only one Fourier component in $z$ is retained, but an arbitrary number of $k_z$'s could be. The second harmonic is the only curl-free term that can contribute in $\rho^2$ order.

The there are four contributions to $\mathcal{T}$ of Equation (B1). $\mathcal{T} = \mathcal{T}_{cc}+\mathcal{T}_{cq}+\mathcal{T}_{qc}+\mathcal{T}_{qq}$ with first suffix denoting $\vec{u}_c$ or $\vec{u}_q$ and the second the corresponding $\delta\vec{B}$.

$$\mathcal{T}_{cc} = 0; \tag{B13}$$

$$\mathcal{T}_{cq} = k_z B_0\frac{\partial(\Delta_{c1}-\Delta_{c2})}{\partial t}\Delta_q\sin(k_z z); \tag{B14}$$

$$\mathcal{T}_{cq} = B_0\frac{\partial\Delta_q}{\partial t}\frac{\partial(\Delta_{c1}-\Delta_{c2})}{\partial z}\cos(k_z z); \tag{B15}$$

$$\mathcal{T}_{qq} = k_z B_0\frac{d\Delta_q^2}{dt}. \tag{B16}$$

Letting $\Delta_{c1}-\Delta_{c2} = \Delta_c(t)\cos(k_z z)+\Delta_s(t)\sin(k_z z)$ gives

$$\mathcal{T} = k_z B_0\left(\frac{d(\Delta_q^2+\Delta_s\Delta_q/2)}{dt}\right) + k_z B_0\Big\{\left(\frac{d\Delta_c}{dt}\Delta_q - \Delta_c\frac{d\Delta_q}{dt}\right)\frac{\sin(2k_z z)}{2} + \left(\Delta_s\frac{d\Delta_q}{dt} - \frac{d\Delta_s}{dt}\Delta_q\right)\frac{\cos(2k_z z)}{2}\Big\}. \tag{B17}$$

When the various $\Delta$'s increase together, so $d\ln\Delta_c/dt = d\ln\Delta_s/dt = d\ln\Delta_q/dt$,

$$\mathcal{T} = k_z B_0\left(\frac{d(\Delta_q^2+\Delta_s\Delta_q/2)}{dt}\right) \quad \text{and} \tag{B18}$$

$$\nu_{hb} = k_z\frac{\Delta_q^2+\Delta_s\Delta_q/2}{2a^2} \tag{B19}$$

is the Huang and Bhattacharjee analogue of $\nu$ in Equation (29) using the coefficients that they used to make their equations dimensionless.

[1] E. N. Parker and M. Krook, *Diffusion and severing of magnetic lines of force*, Ap. J. **124**, 214 (1956): doi10.1086/146216.

[2] M. Hesse and P. A. Cassak, *Magnetic Reconnection in the Space Sciences: Past, Present, and Future*, Journal of Geophysical Research: Space Physics **125**, e2018JA025935 (2020): doi10.1029/2018JA025935.

[3] K. Schindler, M. Hesse, and J. Birn, *General magnetic reconnection, parallel electric-fields, and helicity*, Journal of Geophysical Research—Space Physics **93**, 5547 (1988): doi10.1029/JA093iA06p05547.

[4] H. Ji and J. Karpen with co-authors, *White Paper for Heliophysics 2050: Major Scientific Challenges and Opportunities in Understanding Magnetic Reconnection and Related Explosive Phenomena in Solar and Heliospheric Plasmas*, <https://arxiv.org/pdf/2009.08779.pdf>, Sept. 2020: doi.org/10.48550/arXiv.2009.08779.

[5] A. H. Boozer and T. Elder, *Example of exponentially enhanced magnetic reconnection driven by a spatially bounded and laminar ideal flow*, Phys. Plasmas **28**, 062303 (2021): doi10.1063/5.0039776.

[6] Y.-M. Huang and A. Bhattacharjee, *Do chaotic field lines cause fast reconnection in coronal loops?*, Phys. Plasmas **29**, 122902 (2022): doi10.1063/5.0120512.

[7] H. Aref, *Stirring by chaotic advection*, J. Fluid Mech. **143**, 1 (1984): doi.org/10.1017/S0022112084001233.

[8] X. Z. Tang and A. H. Boozer, *A Lagrangian analysis of advection-diffusion equation for a three dimensional chaotic flow*, Phys. Fluids **11**, 1418 (1999): doi10.1063/1.870006.

[9] Karl Popper, *The Logic of Scientific Discovery*, (Hutchinson & Co, 1959) and *Logik der Forschung*, (Julius Springer,1934).

[10] A. H. Boozer, *Plasma equilibrium with rational magnetic surfaces*, Phys. Fluids **24**, 1999 (1981): doi10.1063/1.863297.

[11] A. H. Boozer, *Magnetic reconnection and thermal equilibration*, Phys. Plasmas **28**, 032102 (2021): doi10.1063/5.0031413.

[12] A. H. Boozer, *Local analysis of fast magnetic reconnection*, Phys. Plasmas **29**, 052104 (2022): doi10.1063/5.0089793.

[13] A. H. Boozer, *Erratum: Local analysis of fast magnetic reconnection*, Phys. Plasmas **30**, 019901: doi10.1063/5.0136708.

[14] D. Borgogno, D. Grasso, F. Porcelli, F. Califano, F. Pegoraro, and D. Farina, *Aspects of three-dimensional magnetic reconnection*, Phys. Plasmas **12**, 032309 (2005): doi10.1063/1.1857912.

[15] A. Lazarian and E. T. Vishniac, *Reconnection in a Weakly Stochastic Field*, Ap. J. **517**, 700 (1999): doi10.1086/307233.

[16] G. L. Eyink, A. Lazarian, and E. T. Vishniac, *Fast magnetic reconnection and spontaneous stochasticity*, Ap. J. **743**, 51 (2011): doi10.1088/0004-637X/743/1/51.

[17] A. Lazarian, G. L. Eyink, A. Jafari, G. Kowal, H. Li, S-Y Xu, and E. T. Vishniac, *3D turbulent reconnection: Theory, tests, and astrophysical implications*, Phys. Plasmas **27**, 012305 (2020): doi10.1063/1.5110603

[18] E. Priest, *MHD structures in three-dimensional reconnection*, *Book Series Astrophysics and Space Science Library*, *Magnetic reconnection: concepts and applications*, volume **427**, page 101 (Springer International Publishing 2016, edited by WalterGonzalez and Eugene Parker): doi10.1007/978-3-319-26432-5-3.

[19] J. Reid, C. E. Parnell, A. W. Hood, and P. K. Browning, *Determining whether the squashing factor, Q, would be a good indicator of reconnection in a resistive MHD experiment devoid of null points*, Astronomy and Astrophysics **633**, A92 (2020): doi10.1051/0004-6361/201936832.

[20] A. H. Boozer, *The rapid destruction of toroidal magnetic surfaces*, Phys. Plasmas **29**, 022301 (2022): doi10.1063/5.0076363.

[21] S. C. Jardin, N. M. Ferraro, W. Guttenfelder, S. M. Kaye, and S. Munaretto, *Ideal MHD Limited Electron Temperature in Spherical Tokamaks*, Phys. Rev. Lett. **128**, 245001 (2022): doi10.1103/PhysRevLett.128.245001.

[22] A. H. Boozer, *Magnetic reconnection with null and X-points*, Phys. Plasmas **26**, 122902 (2019): doi10.1063/1.5121320.

[23] T. Elder and A. H. Boozer, *Magnetic nulls in interacting dipolar fields*, J. Plasma Phys. **87**, 905870225 (2021): doi10.1017/s0022377821000210.

[24] W. A. Newcomb, *Motion of magnetic lines of force*, Ann. Phys. **3**, 347 (1958): doi10.1016/0003-4916(58)90024-1.

[25] A. H. Boozer, *Physics of magnetically confined plasmas*, Rev. Mod. Phys. **76**, 1071 (2004): doi10.1103/RevModPhys.76.1071.

[26] A. H. Boozer, *The interaction of the ITER first wall with magnetic perturbations*, Nucl. Fusion **61**, 046025 (2021): doi10.1088/1741-4326/abe226.

[27] A. Jafari, E. T. Vishniac, G. Kowal, and A. Lazarian, *Stochastic Reconnection for Large Magnetic Prandtl Numbers* Ap. J. **860**, 52 (2018): doi10.3847/1538-4357/aac517.

[28] M. A. Berger, *Rigorous new limits on magnetic helicity dissipation in the solar corona*, Geophysical and Astrophysical Fluid Dynamics, **30**, 79 (1984): doi10.1080/03091928408210078.

[29] A. H. Boozer, *Ohm's Law for mean magnetic fields*, J. Plasma Physics **35**, 133-139 (1986): doi10.1017/S0022377800011181.

[30] A. Bhattacharjee and Y. Yuan, *Self-consistency constraints on the dynamo mechanism*, Ap. J. **449**, 739 (1995): doi10.1086/17609.

[31] F. Rincon, *Dynamo theories*, J. Plasma Phys. **85**, 205850401 (2019): doi10.1017/S0022377819000539.

[32] E. T. Vishniac and J. Cho, *Magnetic Helicity Con-*

*servation and Astrophysical Dynamos*, Ap. J. **550**, 752 (2001): doi10.1086/319817.

[33] J. Heyvaerts and E. R. Priest, *Coronal heating by phase mixed shear Alfvén waves*, Astron. Astrophys. **117**, 220 (1983).

[34] P.L. Similon and R. N. Sudan, *Energy-dissipation of Alfvén-wave packets deformed by irregular magnetic-fields in solar-coronal arches*, Ap. J. **336**, 442 (1989): doi10.1086/167023.

[35] A. H. Boozer *Flattening of the tokamak current profile by a fast magnetic reconnection with implications for the solar corona*, Phys. Plasmas **27**, 102305 (2020): doi10.1063/5.0014107.

[36] D. P. Stern, *The motion of magnetic field lines*, Space Science Reviews **6**, 147 (1966): doi10.1007/BF00222592.

[37] X. Z. Tang and A. H. Boozer, *Anisotropies in magnetic field evolution and local Lyapunov exponents*, Phys. Plasmas **7**, 1113 (2000): 10.1063/1.873919.

[38] J. L. Thiffeault and A. H. Boozer, *The onset of dissipation in the kinematic dynamo*, Phys. Plasmas **10**, 259 (2003): doi10.1063/1.1528902.

[39] R. M. Kulsrud, Y.-C. Sun, N. K. Winsor, and H. A. Fallon, *Runaway electrons in plasma*, Phys. Rev. Lett. **31** 690 (1973): doi10.1103/PhysRevLett.31.690

[40] A. H. Boozer, *Implications of magnetic Helicity conservation*, "Magnetic helicity in space and laboratory plasmas," edited by M. R. Brown and R. C. Canfield (American Geophysical Union, Washington, DC, 1999) p.11-16.

[41] A. H. Boozer, *Particle acceleration and fast magnetic reconnection*, Phys. Plasmas **26**, 082112 (2019); doi10.1063/1.5094179.

[42] P. Song, *A model of the solar chromosphere: structure and internal circulation*, Ap. J. **846**, 92 (2017): doi10.3847/1538-4357/aa85e1.

[43] T. Okamoto and T. Sakurai *Super-strong magnetic field in sunspots*, Ap. J. Lett. **852**, L16 (2018): doi10.3847/2041-8213/aaa3d8.

[44] M. Sobotka and K. G. Puschmann, *Horizontal motions in sunspot penumbrae*, Astronomy and Astrophysics **662**, A13 (2022): doi10.1051/0004-6361/202243577.

[45] M. J. Aschwanden, *Physics of the solar corona*, (Springer 2006, ISBN 3540307656), Section 7.5.

[46] A. H. Boozer, *Runaway electrons and ITER*, Nucl. Fusion **57**, 056018 (2017): doi10.1088/1741-4326/aa6355.

[47] A H. Boozer, *Magnetic reconnection in space*, Phys. Plasmas **19**, 092902 (2012): doi10.1063/1.4754715.

[48] T. S. Kuhn, *The Structure of Scientific Revolutions* (University of Chicago Press, Chicago and London, 1962): ISBN 9780226458113.

[49] Britannica, The Editors of Encyclopaedia (2021, July 14). "Thomas S. Kuhn." Encyclopedia Britannica. https://www.britannica.com/biography/Thomas-S-Kuhn.